

Self-consistent trajectories for surface scattering via classical-quantal coupling

K. J. Schafer, J. D. Garcia, and N.-H. Kwong

Department of Physics, University of Arizona, Tucson, Arizona 85721

(Received 30 January 1987)

We present a set of coupled Schrödinger-Hamiltonian equations that may be solved to give self-consistent classical trajectories and quantal wave functions while conserving total energy and momentum during time-dependent simulations of electronic systems. As a first nontrivial application, we examine the collision of an atom with an infinite barrier. Our results clearly demonstrate the necessity for and importance of classical-quantal coupling in low-energy scattering.

I. INTRODUCTION

The quantum-mechanical calculation of electronic properties during, and as a result of, time-dependent processes often involves a parametrization of the motion of the various nuclei involved.¹ The motion of these nuclei is usually treated classically, because of their large mass, and serves to define all or part of the “external potential” to which the electronic wave functions respond. Treatments of the nuclear motion range from the very simple, e.g., an assumed set of constant velocities, to the more complex, e.g., a classical trajectory derived from an assumed surface potential.

These methods neglect feedback effects from the electronic wave functions to the nuclear trajectory and therefore do not conserve the total system energy or momentum. In this paper we present a method for calculating nuclear trajectories by incorporating the effects of the electronic degrees of freedom directly into the equations of motion for the nuclear coordinates. This allows for a fully self-consistent coupling between classical and quantal particles. We call this classical-quantal coupling (CQC).² We expect that CQC will be important in many low-energy scattering situations (i.e., the “adiabatic” regime), and it is of course crucial in obtaining the correct adiabatic limit of any time-dependent simulation. It also provides a practical intermediate calculation between fully wave-mechanical treatments and classical Monte Carlo calculations.

This paper is organized as follows. In Sec. II we state the CQC equations and discuss their derivation and formal consequences. Section III details the first application of these equations to a nontrivial problem, the scattering of low-energy atoms from an infinite barrier. In addition to illustrating the need for CQC in low-energy calculations, this example also highlights many of the features of time-dependent surface-scattering simulations. In concluding, we indicate a few of the situations for which we expect CQC to be fruitfully applied.

II. THE CQC EQUATIONS

For convenience, we denote classical coordinates by capital letters and quantal coordinates by lower-case letters. Though the CQC equations may be applied to

any quantum many-body system, we shall frequently use “electrons” and “nuclei” as shorthand for quantal and classical particles. In our CQC formulation, the quantal particles evolve via a Schrödinger-like equation for A electrons and N nuclei

$$i\hbar \frac{\partial}{\partial t} \psi = \hat{H}_e \psi(\mathbf{x}_1, \dots, \mathbf{x}_A, t), \quad (1)$$

$$\hat{H}_e = - \sum_i^A \frac{\hbar^2}{2m_i} \nabla_{\mathbf{x}_i}^2 + \sum_i^A \sum_j^N V_{e-n}(X_j(t), \mathbf{x}_i) + \sum_{\substack{i,j \\ (i < j)}}^A V_{e-e}(\mathbf{x}_i, \mathbf{x}_j).$$

The classical coordinates are specified by the Hamiltonian equations

$$\dot{\mathbf{X}}_j = \frac{\mathbf{P}_j}{M_j}, \quad (2a)$$

$$\dot{\mathbf{P}}_j = - \sum_{\substack{i \\ (i \neq j)}}^N \nabla_{\mathbf{X}_j} V_{n-n}(X_i(t), X_j(t)) - \sum_i^A \langle \psi | \nabla_{\mathbf{X}_j} V_{e-n}(\mathbf{X}_j, \mathbf{x}_i) | \psi \rangle. \quad (2b)$$

The simultaneous solution of (1) and (2) gives both ψ and the classical coordinates as functions of time. The last term in Eq. (2b) is the CQC force on the nuclei due to the instantaneous density distribution of electrons.

An immediate consequence of the CQC equations is that for velocity-independent potentials we may define the total energy of the system to be

$$E_{\text{tot}} = \sum_i^N \frac{\mathbf{P}_i^2}{2M_i} + \sum_{\substack{i,j \\ (i < j)}}^N V_{n-n}(X_i(t), X_j(t)) + \langle \psi(t) | \hat{H}_e | \psi(t) \rangle, \quad (3)$$

where \hat{H}_e is the exact electronic Hamiltonian. This quantity is explicitly conserved, as may be seen by differentiating (3) and substituting (1) and (2). The total linear and angular momenta are similarly conserved. We

can thus follow the exchange of energy and momentum between electronic and nuclear coordinates in a self-consistent manner.

The CQC equations can be derived or made plausible in a number of ways. At the level of plausibility one may simply write down Eq. (3) and require energy conservation. It is also possible to derive the CQC equations from a variational principle. We will summarize this derivation here. The full derivation and a detailed analysis are given elsewhere.³

We begin by noting that the exact $(N + A)$ -body Schrödinger equation may be derived by first defining an action

$$\mathcal{F} = \int_{t_0}^{t_1} dt \left\langle \Psi \left| i\hbar \frac{\partial}{\partial t} - \hat{H} \right| \Psi \right\rangle, \quad (4)$$

and then extremizing it over the entire Hilbert space of nuclear and electronic wave functions. Here \hat{H} is the full quantum-mechanical Hamiltonian

$$\hat{H} = - \sum_{i=1}^N \frac{\hbar^2}{2M_i} \nabla_{\mathbf{X}_i}^2 + \sum_{i,j}^N V_{n-n}(X_i(t), X_j(t)) + \hat{H}_e.$$

The CQC equations are obtained when the action (4) is extremized over a restricted set of wave functions of the form

$$\Psi = \phi(X_1(t), \dots, X_N(t), t) e^{i/\hbar S(X_1, \dots, X_N, t)} \times \psi(\mathbf{x}_1, \dots, \mathbf{x}_A, \mathbf{X}_0, t), \quad (5)$$

where the electronic wave functions ψ are correlated to the initial nuclear coordinates, which we denote collectively as \mathbf{X}_0 , only. S is parametrized by the possible nuclear paths and ϕ is a semiclassical amplitude for the nuclear paths.

As a practical matter, one may seek an alternative to the A -body Schrödinger Eq. (1). This can be neatly accomplished by further restricting the electronic wave functions in (5) to be a set of Slater determinants. Equation (1) is then replaced by the well-known time-dependent Hartree-Fock (TDHF) equations which are a set of coupled integro-differential equations for the A -independent single-particle orbitals. It can be shown that all of the conservation principles mentioned above and formulated with the exact Hamiltonian [e.g., Eq. (3)] still hold when the electronic wave functions evolve via the TDHF equations.³

As with any variational calculation, one may state explicitly the conditions necessary for the evolved wave functions to remain in the assumed (restricted) subspace. In our case, these conditions are the usual WKB or eikonal condition that the variation of $\hbar\phi$ is small compared to that of S and a condition related to the smallness of the quantal-to-classical mass ratio. These conditions, detailed elsewhere, must of course be checked *a posteriori* to any actual calculation.

There are a number of important and advantageous reasons for using the form in Eq. (5). A paramount one is that we recover the semiclassical Born-Oppenheimer approximation in the adiabatic limit. Another is its direct transition to eikonal or other high-energy scattering limits.

III. APPLICATION TO HARD-WALL SCATTERING

We consider the scattering of an atom by an infinite barrier. The barrier serves as a boundary condition for the wave-mechanical electrons and as a perfect reflector of the classical nucleus. The barrier may be thought of as a crude model of a simple metal surface, since the surface electrons present a strong, short-range repulsive potential to the incoming electrons via the Pauli exclusion principle, and the heavily screened surface ions (surface atoms minus conduction electrons) present a short-range repulsive potential to the nucleus. Through its simplicity, the barrier model serves to cleanly illustrate the effects of CQC in an unambiguous manner.

We have calculated the time evolution of the scattered atom by starting with a Hartree-Fock ground state far from the barrier, boosting the electronic wave functions to a velocity v_0 and giving the same initial velocity to the nucleus. The CQC equations are then solved on a discretized space-time grid for $\psi(t)$ and for $\mathbf{X}(t)$, the nuclear position, at time intervals Δt . The electronic wave functions are calculated using a TDHF program previously detailed in the literature.⁴ The classical particle trajectory, Eq. (2), is calculated to the same order in Δt as the TDHF equations to obtain properly self-consistent simultaneous solutions of (1) and (2). In all cases considered, the total energy of the system remained accurately constant. For simplicity, we restricted the solution to the case of normal incidence.

A typical trajectory is shown in Fig. 1(a), where the position of a helium nucleus and the average position $\langle z \rangle$ of

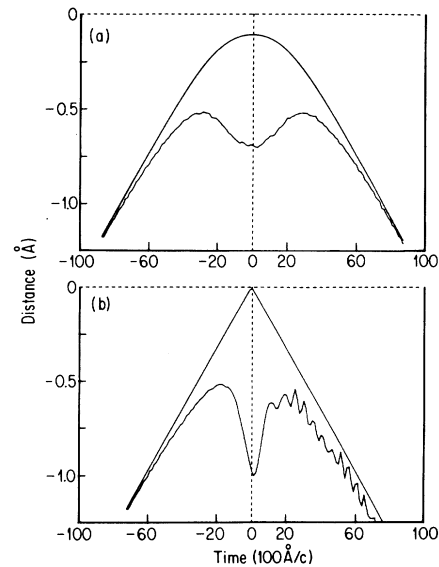


FIG. 1. (a) Upper curve: Nuclear trajectory, $Z(t)$. Lower curve: Average electron coordinate $\langle z \rangle(t)$. Calculation using CQC for a helium atom incident upon a barrier at $Z=0$. The incident energy is $E_0=50$ eV. The nucleus is pulled away from the barrier and the electrons exhibit adiabatic behavior. (b) The same quantities calculated without CQC. The electrons exhibit nonadiabatic behavior due to their lack of feedback to the nuclear trajectory.

the electronic charge density are plotted. The most striking feature is that for the initial kinetic energy used, $E_0 = 50$ eV, the nucleus never comes in contact with the barrier. The distortion of the electron cloud caused by its contact with the barrier is sufficient to cause a 50-eV excitation of the electrons. Since the total energy of the system is conserved, this energy is drained from the nuclear motion; the nucleus is pulled away from the barrier by the electrons. The time symmetry of the curves in Fig. 1(a) are an indication that this is very nearly adiabatic behavior. This was borne out by calculating the adiabatic energy curve for a helium atom in the presence of an infinite barrier as a function of the nuclear distance from the barrier. Although we have made no assumption of adiabaticity in the dynamic simulation, its electronic energy reproduced the adiabatic result. That would not have been possible had we parametrized the nuclear motion. In Fig. 1(b) we show the same quantities as in Fig. 1(a), also calculated using the TDHF program, but assuming that the nuclear velocity is unaffected by the electrons (a common assumption in surface-scattering calculations). The results clearly show that contact with the barrier has induced nonadiabatic behavior.

We have made a more detailed study of the case where hydrogen atoms impinge upon the barrier. For all initial energies below 10.2 eV, the trajectories are similar to Fig. 1(a) with expanded distance and time scales. Again, calculation of the adiabatic energy curve shows that, similar to the helium atom, the adiabatic ground state at the point where the nucleus reaches the barrier is one-half of a $2p$ state aligned along the surface normal with an energy, in this case, 10.2 eV higher than the initial ground state. The adiabatic regime is thus recovered as the low energy limit of our simulation. Dramatic visual confirmation of these results is contained in the time-dependent electronic density contours, which are shown in Fig. 2.

In the energy region above $E_0 = 10$ eV, the nucleus is able to make contact with the barrier and trajectories similar to Fig. 1(b) are calculated. Here again, CQC is necessary for the accurate calculation of electronic properties. The inset on Fig. 3 shows the amount of electronic excitation found in the asymptotic state of a hydrogen atom

$$[\langle \psi | \hat{H}_e | \psi \rangle (t \rightarrow +\infty) - \langle \psi | \hat{H}_e | \psi \rangle (t \rightarrow -\infty)] .$$

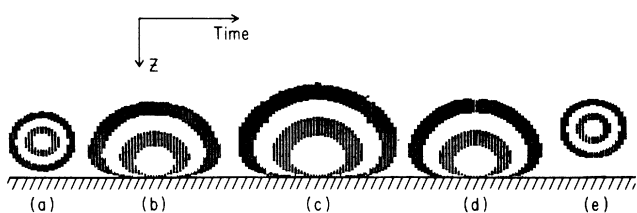


FIG. 2. Density contours of the electronic wave function of a hydrogen atom incident upon a barrier with $E_0 = 10$ eV. The alternating light and dark bands are contours of decreasing density in powers of 10^0 , 10^{-1} , 10^{-2} , and 10^{-3} of the central density. The view shown is a plane perpendicular to the barrier. Time proceeds from (a) to (e) in equal intervals.

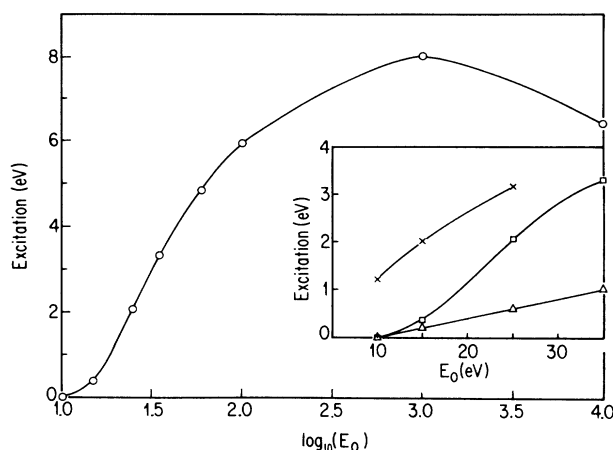


FIG. 3. The amount of asymptotic electronic excitation vs log of incident nuclear energy, calculated with CQC equations for hydrogen incident on an infinite barrier. Shown in the inset are the asymptotic electronic excitation for low incident energies. Upper curve: non-CQC trajectory. Middle curve: CQC trajectory. The lower curve is a perturbative calculation.

The excitation was calculated with and without the CQC force (the middle and upper curves, respectively). The amount of excitation in the diabatic regime is overestimated by the calculation that ignores electronic feedback to the nuclear motion. Even at 25 eV initial energy, 2.5 times the energy at which the adiabaticity begins to give way, CQC is an important factor. The use of self-consistent trajectories is evidently necessary in low-energy time-dependent simulations. If one includes in this simulation a more realistic surface model that allows the surface to respond to the atom, the difference between CQC and non-CQC trajectories for the calculation of energy loss and charge transfer should be substantial. Simulations of this type are currently under way.

From the time-dependent quantities that we have calculated, we can assemble a complete picture of the dynamics of the hydrogen-barrier collision. This serves to illustrate many of the features of time-dependent surface-scattering simulations. In Fig. 4(a) the total and kinetic energy of the electron are plotted as functions of time for the case of $E_0 = 10$ eV. The electron moves along the adiabatic energy surface in this case. As the nucleus approaches the barrier, the electron's kinetic energy first rises and then falls dramatically. The peak in kinetic energy is associated with the point of closest approach of the average electron coordinate to the barrier (the turning point for $\langle z \rangle$ seen clearly in Fig. 1), a distance of about 1.0 Å for hydrogen at low energies. As the electron cloud recedes from the barrier, the kinetic energy falls. At the same time, the density distribution is rapidly expanding, causing the potential energy to rise; the electronic energy rises smoothly throughout the nucleus' approach to the barrier. Asymptotically there is no excitation.

At higher incident energies, such as the 25-eV case illustrated in Fig. 4(b), the electron essentially follows the adiabatic curve on approach to the barrier with over 90%

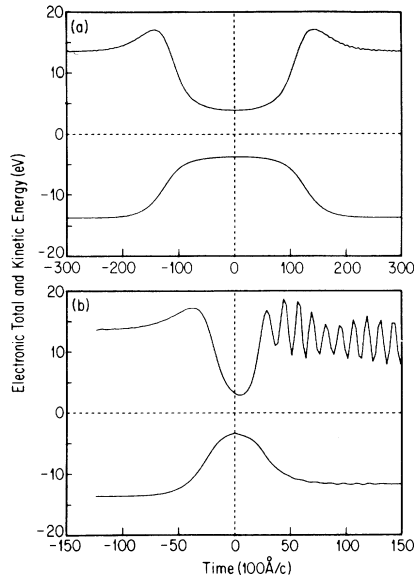


FIG. 4. Electronic kinetic (upper curve) and total (lower curve) energy as functions of time (a) $E_0 = 10$ eV; (b) $E_0 = 25$ eV, both for hydrogen.

of the electron density remaining in the adiabatic ground state up to the time when the nucleus is reflected by the barrier. The sharp, nonelectronically controlled turning of the nucleus induces transitions to excited states, and there is asymptotic excitation of the electron (hence, the asymptotic speed of the nucleus is lower than its initial velocity). Again, striking visual evidence of these conclusions is contained in the time-dependent density contours of Fig. 5. Depending on how fast the nucleus is traveling, the induced transitions may mix only a few states above the ground state. The lowest curve in the inset of Fig. 3 shows a perturbative calculation of the asymptotic excitation, assuming that the reflection of the nucleus mixes the adiabatic ground state with the first excited state for a short time.⁵ It is accurate only at energies just above adiabatic.

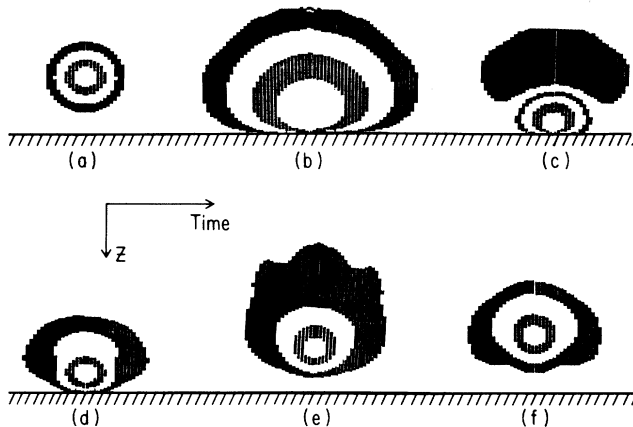


FIG. 5. Same as Fig. 2 with $E_0 = 25$ eV.

Projection of the time-dependent wave function onto translating hydrogen-bound states reveals that the first excited state is coherently mixed with the ground state as the atom leaves the barrier region. This is responsible for the definite periodicity of the oscillations in the total kinetic energy after the collision in Fig. 4(b). The asymptotic period corresponds to a 10.2-eV separation of these levels. The projection of the asymptotic wave function onto free-space hydrogenic orbitals is plotted in Fig. 6 versus the log of the incident nuclear energy. The projection onto a level n is given by the incoherent sum

$$P(n) = \sum_{l,m} |\langle nlm | \psi(t \rightarrow \infty) \rangle|^2. \quad (6)$$

At low energies, the asymptotic state consists of mostly the ground state and the first two excited levels. The probability of exciting $n=2$ or $n=3$ level orbitals has a peak in the energy region around a few hundred eV. At higher incident energy, the excitation has a larger ionization component with only a $1s$ "core" remaining around the nucleus.

As the incident energy rises to an order of magnitude above the binding energy, the details of the nuclear motion become less important; we find that CQC has only negligible effects for incident energies above a few hundred eV. We note that the asymptotic electronic excitation for the range of incident energies 10 eV to 10 keV, shown in Fig. 3, exhibits a peak around 1 keV. At higher energies it is presumably harder to excite the electron because the atom enters and leaves the region near the barrier in a time interval much shorter than a typical electronic response time.

IV. CONCLUSION

We have demonstrated in this paper a method for generating self-consistent nuclear trajectories which are coupled to solutions of the time-dependent Schrödinger equation. The collision of atoms with an infinite barrier illustrates the necessity of this technique for low-energy

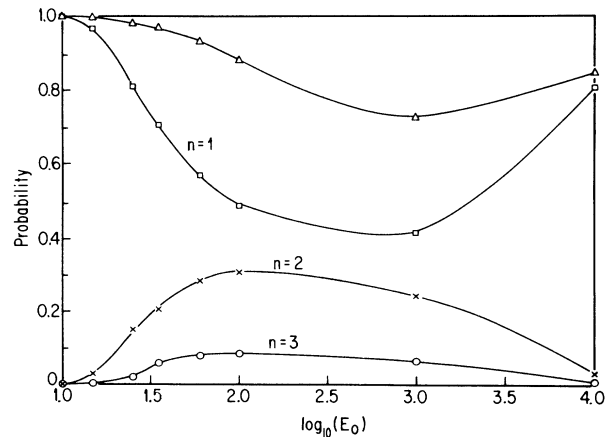


FIG. 6. Asymptotic probabilities for $n=1, 2$, and 3 levels vs log of incident nuclear energy for hydrogen incident on an infinite barrier. The top curve is the sum of the lower three.

scattering. The fact that our CQC approximation allows for the conservation of total energy was crucial. The use of CQC and TDHF methods allows us to calculate all of the atomic parameters as a function of time across the entire range of incident energies within a single technique.

The conservation of linear and angular momenta within the CQC scheme may also be important in more realistic low-energy scattering simulations. There are also many calculations where initially free intermediate or heavy particles interact with a system of electrons. Examples include the recombination of antiprotons via atomic collision and the capture of negative muons by hydrogen. These calculations have been done either by treating all of the particles quantum mechanically or classically via Monte Carlo methods. CQC provides an alternative whereby all of the important system quantities can be

conserved and the mass ratio of heavy or intermediate particles to electrons can be efficiently exploited. The resulting mix of classical and quantum-mechanical particles will include most of the important wave-mechanical effects and yet be considerably simpler to simulate than the full-wave mechanical system. Calculations of this type are also currently under way.

ACKNOWLEDGMENTS

This work was supported in part by the National Science Foundation (NSF), Grant No. PHY84-01694. The computations were carried out on the Minnesota Supercomputer Center (MSC) Cray 2 using NSF allocated time. The assistance of the MSC technical staff is gratefully acknowledged.

¹J. C. Tully, Phys. Rev. B **16**, 4324 (1977); R. Brako and D. M. Newns, Surf. Sci. **108**, 253 (1981); J. A. Appelbaum and D. R. Hamann, Phys. Rev. B **12**, 5590 (1975).

²R. C. Sorbello [Phys. Rev. A **30**, 683 (1984)] included some nuclear response in a first-order calculation of an atom in an electric field. No attempt at self-consistency was made.

³N.-H. Kwong, J. Phys. B (to be published).

⁴K. C. Kulander, K. R. Sandya Devi, and S. E. Koonin, Phys. Rev. A **25**, 2968 (1982); K. R. Sandya Devi and J. D. Garcia, J. Phys. B **16**, 2837 (1983).

⁵N. F. Mott and H. S. W. Massey, *The Theory of Atomic Collisions* (Oxford University Press, London, 1965), p. 793.